HHS Public Access

Author manuscript

Dev Biol. Author manuscript; available in PMC 2018 March 15.

Published in final edited form as:

Dev Biol. 2017 March 15; 423(2): 126–137. doi:10.1016/j.ydbio.2017.01.020.

Celsr1 Coordinates the Planar Polarity of Vestibular Hair Cells During Inner Ear Development

Jeremy S. Duncan[1,2,1], **Michelle L. Stoller**[1,2,1], **Andrew F. Francl**[1,2], **Fadel Tissir**[3], **Danelle Devenport**[4], and **Michael R. Deans**[1,2,*]

[1]Department of Surgery, Division of Otolaryngology, University of Utah School of Medicine, Salt Lake City, UT, USA

[2]Department of Neurobiology & Anatomy, University of Utah School of Medicine, Salt Lake City, UT, USA

[3]Institute of Neuroscience, Université Catholique de Louvain, Brussels, Belgium

[4]Department of Molecular Biology, Princeton University, Princeton, NJ, USA

Abstract

Vestibular hair cells of the inner ear are specialized receptors that detect mechanical stimuli from gravity and motion via the deflection of a polarized bundle of stereocilia located on their apical cell surfaces. The orientation of stereociliary bundles is coordinated between neighboring cells by core PCP proteins including the large adhesive G-protein coupled receptor Celsr1. We show that mice lacking Celsr1 have vestibular behavioral phenotypes including circling. In addition, we show that Celsr1 is asymmetrically distributed at cell boundaries between hair cells and neighboring supporting cells in the developing vestibular and auditory sensory epithelia. In the absence of Celsr1 the stereociliary bundles of vestibular hair cells are misoriented relative to their neighbors, a phenotype that is greatest in the cristae of the semicircular canals. Since horizontal semi-circular canal defects lead to circling in other mutant mouse lines, we propose that this PCP phenotype is the cellular basis of the circling behavior in *Celsr1* mutants.

Introduction

Vestibular hair cells of the inner ear are sensory receptors that convert mechanical stimuli triggered by gravity or motion into neural activity. This information is conducted centrally to control eye position, balance, blood pressure and heart rate (Uchino and Kushiro, 2011; Yates et al., 2014). Hair cell function is dependent upon the development of a polarized structure called the stereociliary bundle, the orientation of which is tightly coordinated between neighboring cells. Gravity or motion are detected via deflections of the stereociliary bundle which is comprised of specialized microvilli, called stereocilia, projecting from the

*Correspondence should be addressed to MRD at michael.deans@utah.edu.
[1]These authors made equal contributions

apical cell surface. The organization of stereocilia in this bundle has a distinct morphological polarity because individual stereocilia are arranged in rows of increasing height with the tallest stereocilia adjacent to a microtubule based kinocilium. In each hair cell, the kinocilium and its associated basal body are laterally displaced to one side of the apical cell surface, and together the rows of stereocilia and the lateral position of the kinocilium forms a morphological polarity axis (Figure 1 and (Deans, 2013)). This is functionally significant because mechanical stimuli that deflect the bundle towards the kinocilium places tension on tip-links interconnecting the stereocilia which opens mechanoelectrical transducer (MET) channels. MET activation depolarizes the hair cell and initiates synaptic transmission to afferent neurons projecting centrally through the eighth cranial nerve (Schwander et al., 2010). In contrast, deflections of the bundle away from the kinocilium releases tip-link tension, decreasing MET open probability and are thus inhibitory. As a result hair cells have a physiological polarity axis that mirrors the morphological polarity axis of the stereociliary bundle (Shotwell et al., 1981).

Vestibular hair cells are located in two sets of sensory organs. The three semi-circular canal cristae which respond to head rotation and the utricular and saccular maculae which respond to linear acceleration and gravity. Auditory hair cells have similar stereociliary bundle structures, respond to acoustic stimuli, and are located in the organ of Corti which spirals along the length of the cochlea (Figure 1). Within a semi-circular canal crista, all hair cell stereociliary bundles are oriented in the same direction and are aligned parallel to the motion of fluid within the canals. As a result, the rotational movement detected by the cristae is determined by the orientation of the semi-circular canal within the temporal bone, and all hair cells of a single cristae are simultaneously activated by head rotations along that plane. In contrast, vestibular hair cells in the utricular and saccular maculae are divided between two groups, each containing hair cells with stereociliary bundles arranged in opposite directions. The position where these two groups meet is a single cell boundary often referred to as the Line of Polarity Reversal (LPR). As a result of this organization, the utricle and saccule each have two populations of hair cells tuned to detect gravity or linear acceleration in opposite directions (Deans, 2013).

The organization of polarized cellular structures between neighboring cells in the plane of an epithelium is called planar cell polarity (PCP) and is evident in many vertebrate systems including auditory hair cells of cochlea and hair follicles in the skin (Goodrich and Strutt, 2011; Wang and Nathans, 2007). Pioneering studies in *D. melanogaster* based upon the development of analogous polarized structures led to identification of core PCP proteins that are required for coordinating structures like wing hairs between neighboring cells (Simons and Mlodzik, 2008; Vladar et al., 2009). The core PCP proteins include the transmembrane receptor Frizzled and its cytoplasmic effector Dishevelled, in addition to the transmembrane protein Vang and its binding partner Prickle. In the developing wing these two sets of PCP proteins are distributed to opposite sides of wing epithelial cells with Frizzled and Dishevelled enriched on the distal side, and Vang and Prickle on the proximal side. At both of these cell boundaries is an adhesive G-protein coupled receptor called Flamingo (Chae et al., 1999; Lu et al., 1999; Usui et al., 1999) that stabilizes the complexes and acts as an intercellular bridge to facilitate the propagation of PCP signaling between cells (Chen et al.,

2008; Struhl et al., 2012; Strutt and Strutt, 2008). The net result is a hair extending from the distal side of the cell and projecting towards the wing tip.

A number of recent studies have demonstrated a conservation of core PCP protein function between *D. melanogaster* wing hairs and inner ear hair cells. For example, mutations in the vertebrate ortholog of Flamingo, a molecule called Celsr1 (Cadherin EGF LAG Seven-pass G-type Receptor 1), results in misoriented auditory hair cell stereociliary bundles (Curtin et al., 2003). Similarly *Vangl2*, which encodes a vertebrate ortholog of the Vang protein, is necessary for the development of auditory and vestibular hair cell PCP (Copley et al., 2013; Montcouquiol et al., 2003; Torban et al., 2008; Yin et al., 2012), and the vertebrate *Frizzled3* (Fz3) and *Frizzled6* (Fz6) genes act redundantly to coordinate stereociliary bundle orientation between neighboring hair cells (Wang et al., 2006b). In addition to conserved gene function, the vertebrate PCP proteins are also asymmetrically distributed within cells in patterns that are highly similarly to analogous *Drosophila* systems (Deans et al., 2007; Giese et al., 2012; Wang et al., 2006b). However, an important difference is that vertebrate hair cells are isolated from their neighbors by intervening supporting cells and thus within the inner ear PCP proteins are enriched at hair cell to supporting cell (HC:SC) or supporting cell to supporting cell (SC:SC) boundaries rather than between hair cells (Deans, 2013).

There are three Celsr proteins encoded by the mouse genome (Celsr1, Celsr2, Celsr3) (Tissir and Goffinet, 2013), and one of the first vertebrate PCP phenotypes was described for two *Celsr1* mutant lines generated by ENU mutagenesis called *spin cycle* and *crash* (Curtin et al., 2003). Consistent with Celsr1 function as a core PCP protein, *spin cycle* and *crash* homozygotes have misoriented auditory hair cells and craniorachischisis; a severe neural tube defect that is present in other PCP mutants such as *Looptail* (Greene et al., 2009; Montcouquiol et al., 2003). In heterozygous mice these mutations also result in vestibular behavioral deficits including head shaking and spinning during vertical tail suspension (Curtin et al., 2003). However, while mice with head shaking or spinning phenotypes often have peripheral vestibular deficits, no vestibular abnormalities were reported for *spin cycle* or *crash* heterozygotes (Curtin et al., 2003). In order to test the possibility that Celsr1 also contributes to peripheral vestibular system development and function, the distribution of Celsr1 protein was evaluated in inner ear sensory organs, and the planar polarity organization of vestibular hair cells and vestibular behavioral phenotypes were evaluated in a *Celsr1* KO line (Ravni et al., 2009).

Results

Celsr1 KO mice have behavior phenotypes indicative of vestibular dysfunction

The *Celsr1* KO mice were generated through a targeted mutagenesis strategy in which deletion of coding sequence exons 26 through 29 removed Celsr1 transmembrane domains 5–7, and introduced a frameshift and premature stop that prevents translation of the cytoplasmic domain. The majority of *Celsr1* KO mice are not viable, with approximately 20% dying *in utero* due to variable neural tube defects, and upwards to half of the remaining mutants dying before weaning (Ravni et al., 2009). The occurrence of neural tube defects in *Celsr1* KOs is consistent with a role of PCP signaling in neural tube closure (Copp et al., 2003). Mice that do survive beyond weaning are smaller than littermate controls and have

characteristic PCP patterning phenotypes in the skin such as hair whirls and crests (Ravni et al., 2009). This is in contrast to the *Celsr1* ENU-mutagenesis lines *spin cycle* and *crash* which are not viable because 100% of homozygous mutants exhibit craniorachischisis (Curtin et al., 2003). In addition to these previously described phenotypes, *Celsr1* KO mice that survive to adulthood have behavioral phenotypes that are frequently associated with inner ear deficits. These include bouts of circling that disrupt linear travel (Figure 2 and Supplemental Movie 1) and occasional headtossing or headbobbing motions. This is consistent with the behaviors reported for *spin cycle* and *crash* heterozygotes (Curtin et al., 2003), and are behavioral phenotypes commonly associated with inner ear and hair cell deficits (Dong et al., 2002; Gibson et al., 1995).

Celsr1 protein is asymmetrically distributed at cell boundaries during inner ear development

A distinctive feature of PCP in vertebrates and invertebrates is the asymmetric distribution of core PCP proteins at cell boundaries. This has been demonstrated in the mouse for Vangl2, Fz3, Fz6 and Prickle2 (Pk2) in the organ of Corti of the cochlea and in the utricular macula (Deans et al., 2007; Montcouquiol et al., 2006; Wang et al., 2006b). In the utricle, Pk2 is highly enriched along one side of vestibular hair cells where they contact adjacent supporting cells. This distinctive pattern revealed that the relative distribution of PCP protein complexes is constant throughout the maculae and does not change between hair cells located on opposite sides of the LPR (Deans et al., 2007). Thus the core PCP proteins appear to form an underlying ground polarity that coordinates the orientation of stereociliary bundles between neighboring hair cells, but are not positioned to directly contribute to polarization of the bundle or formation of the LPR.

The distribution of Celsr1 was evaluated in the mouse sensory epithelia using an antibody against amino acids 2885–2985 that recognizes an antigen in the cytoplasmic domain (Devenport and Fuchs, 2008). Previously a Celsr1 homolog has been visualized at cell junctions in the developing basilar papillae, the auditory sensory epithelia of the chick inner ear (Davies et al., 2005). Here it is enriched at cell boundaries in a pattern that is reminiscent of the distribution of Flamingo protein in *D. melanogaster* and is consistent with protein localization to PCP protein complexes on both the medial and lateral sides of developing hair cells. In the postnatal mouse cochlea Celsr1 distribution is more similar to Vangl2 (Giese et al., 2012), Fz3 and Fz6 (Wang et al., 2006b), and is enriched at the apical cell surface of outer hair cells, along the neural cell boundary where they contact adjacent supporting cells while being less prominent on the abneural side (Figure 3). This is in contrast to Celsr distribution in the chick basilar papillae where protein is enriched on both sides of auditory hair cells (Davies et al., 2005). This difference may reflect the diversity of supporting cells in the mouse organ of Corti which have developed specialized structural morphologies that contribute to the biomechanical properties of the cochlea. In the mouse, Celsr1 is present at the boundaries between the third row of outer hair cells (OHC3) and the adjacent Deiters' cell (DC1), OHC2 and Outer Pillar Cells (OPC), and the boundary between OHC1 and the Inner Pillar Cells (IPC) (Figure 3). Celsr1 is also present neural side of Inner Hair cells (IHC) although there is significantly less protein in IHCs than OHCs. In comparison, Celsr1 is more prominent at the junctions between supporting cells that flank

the IHCs including the junctions between OPCs and IPCs, Interphalangeal Cells (IphC) and IPCs, and IphCs and Border Cells. Finally, Celsr1 can also be found at the junction between the second and third rows of Deiters' cells (DC2 and DC3) and along the abneural side of DC3 (Figure 3). This distribution pattern is constant throughout the length of the cochlea (data not shown), and since hair cells differentiate in a graded sequence from the base to the apex this suggests that the distribution of Celsr1 in the cochlea does not change significantly over developmental time.

In the semi-circular canal cristae Celsr1 has a polarized distribution that is apparent at hair cell to supporting cell (HC:SC) and supporting cell to supporting cell (SC:SC) junctions (Figure 4). While Celsr1 is enriched at HC:SC boundaries and along one side of the hair cell in the cristae (Figure 4B), surprisingly in some locations Celsr1 does not appear to be polarized but rather surrounds individual hair cells (Figure 4C). Despite this variation at HC:SC junctions, Celsr1 maintains a distinct polarized distribution at SC:SC junctions throughout the cristae (Figure 4). Furthermore, this distribution is maintained in the eminentia cruciatum (Figure 4D), a unique region comprised of non-sensory epithelial cells that bisects the sensory region of the anterior and posterior semicircular canal cristae (Figure 1&4A).

Celsr1 is similarly enriched at HC:SC and SC:SC boundaries in the developing utricular maculae although this protein distribution shows greater regional variation and developmental dynamics than Celsr1 in the cristae or organ of Corti. At embryonic day 14.5 (E14.5) the LPR is not evident in the developing utricle because hair cells are differentiating and beginning to organize polarized stereociliary bundles in the medial region while differentiation in the lateral region occurs a day later (Figure 5A). Nonetheless Celsr1 is asymmetrically distributed at cell boundaries in both regions at this stage. In the medial region Celsr1 is enriched at HC:SC boundaries and SC:SC boundaries which can be distinguished based upon cellular morphology following phalloidin stain (Figure 5B). In the lateral region Celsr1 is less organized but is still present at cell boundaries throughout (Figure 5C). Since hair cells are undergoing terminal differentiation and are actively differentiating throughout the utricle at this stage it can be concluded that Celsr1 is present at cell boundaries before stereociliary bundle polarization and therefore is positioned to contribute to this event.

At E17.5 the LPR can be identified based upon morphological criteria, and at this stage Celsr1 is present at HC:SC boundaries (Figure 5D–F, arrowheads) in addition to SC:SC boundaries (Figure 5D–F, arrows). Furthermore the distribution of Celsr1 shows important regional variation throughout the utricular sensory epithelia at this stage. In the medial extrastriolar region, Celsr1 can be detected on both the medial and lateral sides of vestibular hair cells (Figure 5D, arrowheads) which is unique from the organ of Corti (Figure 3) or Cristae (Figure 4), and is more similar to the chick basilar papillae (Davies et al., 2005). In contrast, in the striolar region Celsr1 is also enriched at HC:SC boundaries, however in the striola it is only present at the medial side of the hair cell where it is opposite of the fonticulus and therefore the kinocilium (Figure 5E, arrowheads). Celsr1 is also restricted to one HC:SC boundary in the lateral extrastriolar region where hair cells have the opposite stereociliary bundle orientation than hair cells from the striolar and medial extrastriolar

regions. However, in the lateral extrastriolar region Celsr1 remains enriched on the medial side of hair cells and therefore is adjacent to the fonticulus and hence the kinocilium (Figure 5F, arrowheads). This protein distribution is similar to that previously reported for Pk2 in that Celsr1 and Pk2 are both enriched opposite of the kinocilium in the striolar region and are adjacent to the kinocilium in the lateral extrastriolar region.

During subsequent stages of postnatal development, the distribution of Celsr1 at cell boundaries is dynamic, and is down-regulated at HC:SC boundaries and enriched at SC:SC boundaries. As a result, at P2 Celsr1 becomes restricted to one side of hair cells throughout the utricle (Figure 5G–I) and is severely down-regulated or lost from HC:SC junctions by P5 (Figure 5J–L). Despite this Celsr1 is maintained at SC:SC junctions, and often appears to be enriched at these cell boundaries at P5 compared to E17.5.

The coordinated distribution of Celsr1 between neighboring cells requires PCP signaling

The early molecular polarization of core PCP proteins in *D. melanogaster*, and Pk2 in the mouse inner ear, requires the coordinated activity other core PCP proteins including Vangl1/Vangl2 (Bastock et al., 2003; Deans et al., 2007). To determine if Vangl2 is required for the asymmetric distribution of Celsr1, immunolabeling was conducted on *Pax2*-Cre; *Vangl2* CKO mice where conditional gene deletion results in misoriented hair cells in the striolar region of the utricle (Figure 6 and (Copley et al., 2013)). In the absence of *Vangl2*, Celsr1 distribution remains enriched at apical cell surfaces however the polarized distribution is no longer coordinated between neighboring cells (Figure 6A–D). Moreover, at E17.5 Celsr1 remained enriched at one HC:SC boundary which was always located at the side of the cell opposite of the kinocilium (Figure 6A–B,E–F). Changes in the relative distribution of Celsr1 are not observed in lateral extrastriolar regions where hair cells are not affected by *Pax2*-Cre mediated gene deletion (Copley et al., 2013). Nonetheless these experiments demonstrate that the enrichment of Celsr1 at one HC:SC boundary is correlated with individual hair cell stereociliary bundle polarity, and occurs opposite of the kinocilium in the striolar region (Figure 6C–D). In addition, unlike Pk2, Celsr1 does not require Vangl2 to become established or maintain an asymmetric distribution at cell boundaries. Moreover, in *Pax2*-Cre; *Vangl1; Vangl2* CKO mice in which both of the mouse Vangl genes are disrupted and hair cells are misoriented throughout the utricle, Celsr1 can still be detected at cell boundaries with an asymmetric cellular distribution (Figure 7). Thus while the localization of Celsr1 to cell boundaries does not require PCP signaling, the coordinated organization of Celsr1 at cell boundaries along a tissue polarity axis does require core PCP signaling components.

Celsr1 is Required for Vestibular Hair Cell PCP

The *spin cycle* and *crash* mutations in *Celsr1* each result in behavior phenotypes in heterozygous mice that are suggestive of vestibular deficits and homozygous mutants have craniorachischisis which is indicative of disrupted PCP signaling (Copp et al., 2003; Curtin et al., 2003). In contrast to these homozygous mutants, a portion of *Celsr1* KO mice survive beyond weaning, and neural tube defects only occur in <20% of *Celsr1* KOs (Ravni et al., 2009). Nonetheless mice that survive to adulthood have behavioral phenotypes, including circling, that are consistent with inner ear vestibular deficits (Figure 2). To assess the

possibility that *Celsr1* mutations could yield hair cell PCP phenotypes that underlie these behaviors, hair cell stereociliary bundle orientation was evaluated in each of the inner ear sensory organs. Auditory hair cells of the organ of Corti were immunolabeled using antibodies against β2-Spectrin to visualize the cuticular plate, an actin-rich structure that anchors the stereociliary bundles on the apical hair cell surface, and phalloidin to label the stereociliary bundle (Figure 8). Auditory hair cell PCP is not significantly altered at P0 in Celsr1 KO mice with only 3.2% of OHCs (709 total) having stereociliary bundles that deviated from the neural:abneural axis by >30 degrees in the middle turn of the cochlea (Figure 8B,E) and no OHCs (612 total) affected to this extent in the basal turn (Figure 8A,D). This is in contrast to the *spin cycle* and *crash* mutants in which a large proportion of auditory hair cells appear misoriented in homozygous mutants (Curtin et al., 2003). Moreover, in the extreme apex of the cochlea where OHCs are still differentiating, the *Celsr1* KO cochlea does not show other PCP phenotypes such as extra rows of outer hair cells which have been attributed to convergent extension defects (Figure 8C,F).

Hair cells from the utricular maculae were similarly evaluated for planar polarity defects by immunolabeling with β2-Spectrin alone. The orientation of individual hair cells was measured and quantified on circular histograms for three regions of the utricle corresponding to the striolar and the lateral and medial extrastriolar regions (Figure 9A). These three analysis fields were utilized so that cells could be evaluated from either side of the LPR, and because in *Vangl2* KOs the PCP phenotype is restricted to the striola (Yin et al., 2012). The boundaries of the striolar region were determined by immunolabeling for Oncomodulin as previously described (data not shown) (Copley et al., 2013). In the utricle of *Celsr1* KO mice, vestibular hair cells are still capable of forming polarized stereociliary bundles as evident by the asymmetric position of the fonticulus in all cells (Figure 9B,D). A broader range of stereociliary bundle orientations was detected in all fields, however the general organization of bundles in the epithelia was maintained (Figure 9C,E). Similar to *Vangl2* CKOs, hair cells within the striolar region of the *Celsr1* mutant showed the greatest effect, and these cells were frequently not properly oriented towards the LPR and appeared less organized than in littermate controls (Figure 9D,E). While they did not appear random like *Vangl2* mutants (Copley et al., 2013; Yin et al., 2012), the cells in the striolar region tended to be oriented more posteriorly than controls, and tended to align parallel to the LPR (Figure 9E). In comparison, hair cells in the lateral extrastriolar region maintained a greater degree of organization and as a result the position of the LPR could still be identified in *Celsr1* KOs.

In comparison to the organization of hair cells in the utricle, hair cells in the semi-circular canal cristae showed stronger PCP phenotypes based upon cuticular plate morphology (Figure 10) and measurements of stereociliary bundle orientation (Figure 11). In the horizontal, anterior and posterior semicircular canals cristae, individual hair cells formed asymmetric stereociliary bundles based upon the asymmetric distribution of the fonticulus, however measurement and quantification of bundle orientation revealed a range of orientations that were not coordinated between neighboring cells, or arranged in a single direction that was aligned with the associated semi-circular canal (Figures 10&11). This is significant because hair cells of the cristae are arranged to detect rotational accelerations aligned in the same plane as their semi-circular canal. Therefore, induction of a uniform hair

cell response to rotational motion is likely disrupted in *Celsr1* KO cristae because the organization of stereociliary bundles appears randomized. Of particular interest is the horizontal cristae because defects in horizontal canal development have been associated with circling behavior in other mutants (Abraira et al., 2008). Altogether these phenotypical analyses are consistent with the hypothesis that developmental defects in the semi-circular canal cristae of *Celsr1* KOs lead to circling behaviors in *Celsr1* KO mice.

Discussion

Using antibodies against the adhesion G-protein coupled receptor Celsr1, and by evaluating the vestibular phenotype of *Celsr1* knockout mice we have further demonstrated the conservation of core PCP protein function between *D. melanogaster* and the inner ear hair cells of the mouse that facilitate hearing and balance. In the inner ear Celsr1 is asymmetrically localized at cell boundaries formed between hair cells and the supporting cells that surround them, and is further enriched at cell boundaries between supporting cells. This distribution is consistent with models in which PCP proteins signal from cell to cell in a bucket brigade-like fashion to coordinate the orientation of polarized structures between neighbors. One important difference between the *Drosophila* and inner ear systems is that in the ear signal propagation must pass through an intervening population of supporting cells which themselves do not display overt anatomic features of planar polarization. However, the asymmetric distribution of Celsr1 reveals that these supporting cell populations are indeed polarized at the molecular level. Moreover, in the utricular macula planar polarity appears to persist through postnatal development via Celsr1 enrichment at SC:SC junctions long after Celsr1 is downregulated at HC:SC boundaries (Figure 5).

It is striking to note that in all of the mouse core PCP mutants that have been evaluated to date, the primary phenotype is that stereociliary bundle orientation is not coordinated between neighboring hair cells, yet individual cells are still capable of forming polarized stereociliary bundles (Lu et al., 2004; Montcouquiol et al., 2003; Wang et al., 2006a; Wang et al., 2006b; Yin et al., 2012). We have found that this is also the case for *Celsr1* mutants. This is consistent with work from other labs showing that intracellular planar polarity and polarization of the stereociliary bundle is independently regulated through signaling by Gαi proteins (Ezan et al., 2013; Tarchini et al., 2013). This is also in agreement with a three tiered model of vestibular hair cell development in which the primary function of the core PCP proteins is to establish an underlying polarity axis that aligns adjacent hair cells, and does so irrespective of their position on either side of the LPR (Deans, 2013; Deans et al., 2007). Indeed, Celsr1 is enriched on the medial side of hair cells in both the striolar and lateral extrastriolar regions of the developing utricle which are separated by the LPR. Since the hair cells in these two regions have opposite stereociliary bundle orientations, Celsr1 is opposite of the kinocilium in the striolar region and adjacent to the kinocilium in the lateral extrastriolar region. This pattern is similar to the core PCP protein Pk2. However, we also find that in *Vangl2* CKOs where PCP signaling is disrupted in the striola, Celsr1 remains enriched on the cell boundary opposite of the kinocilium even if the hair cell is incorrectly oriented for that position in the epithelia (Figure 6C&D). One explanation for this coordination might be that Celsr1 is a molecular link between the PCP and Gαi signaling pathways and functions to couple polarization of the stereociliary bundle with an underlying

PCP-dependent ground polarity (Deans, 2013). However, when core PCP signaling is completely disrupted by deleting *Vangl1* and *Vangl2* (Song et al., 2010; Wang et al., 2016), Celsr1 can still be detected at cell boundaries (Figure 7) and this distribution is no longer correlated with either the position of the kinocilium or a planar polarity axis within the tissue. Thus the mechanism linking intracellular planar polarity with the core PCP polarity axis remains uncertain.

Celsr1 was first linked to inner ear PCP for auditory hair cells in the *spin cycle* and *crash* mutant mice. In these lines, independent ENU generated missense mutations in the extracellular cadherin domains of Celsr1 yielded heterozygous mice with vestibular behavior phenotypes and misoriented auditory hair cells. No clear defects in the peripheral vestibular system were found in adult heterozygotes, however homozygous *spin cycle* and *crash* mice have craniorachischisis and auditory hair cell phenotypes similar to other core PCP mutants (Curtin et al., 2003). In this study we find distinct PCP phenotypes in the vestibular sensory organs of *Celsr1* KO mice that are correlated with profound bouts of circling that disrupt mutant mouse navigation throughout the cage but no significant auditory hair cell phenotype. The molecular bass for the different, complementary auditory and vestibular phenotypes that occur in the *Celsr1* ENU mutants and the *Celsr1* knockouts are unclear. One possibility is that the *Celsr1* KO lacks an auditory phenotype because of compensation from other *Celsr* genes (Tissir and Goffinet, 2006, 2013) and therefore has only partially penetrant mutant phenotypes. This could also explain other aspects of the KO phenotype, like neural tube defects, which are less frequent in the *Celsr1* KO than for the *spin cycle* and *crash* mutants. Along these lines, the ENU-induced mutations in the *spin cycle* and *crash* mice are likely to be semi-dominant and as a result generate more pronounced homozygous mutant phenotypes in the organ of Corti than the *Celsr1* KO. This latter explanation would also be consistent with the vestibular behavioral phenotype that epitomizes the *spin cycle* and *crash* heterozygotes. In this case perhaps vestibular hair cell phenotypes may have been overlooked in the *spin cycle* and *crash* heterozygotes because they were restricted to hair cells of the cristae, which still extend stereocilia and are present in normal numbers, but could have subtle changes in stereociliary bundle orientation that are best revealed when analyzed at the cuticular plate. Regardless of the molecular basis for these differences, the *Celsr1* mutant phenotype in the semi-circular canal cristae likely underlies the behavioral phenotype because mice in which the semi-circular canals fail to form properly also circle (Abraira et al., 2008; Cryns et al., 2004). Moreover, in the cristae it is essential that the stereociliary bundles are properly aligned with the associated semi-circular canals in order for the hair cells to be stimulated by rotational movements. Thus a simple explanation is that *Celsr1* KO mice circle because stereociliary bundles within the horizontal cristae are poorly aligned with the horizontal semi-circular canal, and that headtossing and headbobbing are similarly due to disorganization in the anterior and posterior cristae. However since this is a global knockout, inner ear restricted CKOs would be needed to confirm these hypotheses.

Materials and Methods

Mouse husbandry and genotyping

Pax2-Cre; *Vangl2* CKO were produced by intercrossing *Pax2*-Cre+; *Vangl2* $^{\Delta TMs/WT}$ male mice with *Vangl2* ^{Floxed} female mice as previously described (Copley et al., 2013). *Pax2*-Cre; *Vangl1; Vangl2* CKO mice were produced by intercrossing *Pax2*-Cre; *Vangl1* $^{\Delta TMs/WT}$; *Vangl2* $^{\Delta TMs/WT}$ male mice with *Vangl1* ^{Floxed}; *Vangl2* ^{Floxed} female mice. The *Pax2-Cre* line (Ohyama and Groves, 2004) were provided by Andrew Groves (Baylor College of Medicine). The Vangl1 mouse line was generously provided by J. Nathans (Johns Hopkins University School of Medicine) and have been previously characterized (Wang et al., 2016). For colony preservation all mouse lines were back-crossed with hybrid B6129SF1/J females (Jackson strain #101043). CD1 mice were obtained from Charles River (Strain# 022) and used for wild type Celsr1 experiments. For timed breeding and tissue staging, noon on the day of vaginal plug visualization was considered embryonic day 0.5 (E0.5), and postnatal day 0 (P0) was the day mice were born. CD1, *Vangl1*, *Vangl2*, and *Pax2*-Cre mice were maintained at the University of Utah under IACUC approved guidelines. *Celsr1* mutant and littermate control tissue was provided by F. Tissir and the *Celsr1* mouse line was maintained at the Université Catholique de Louvain under institutional guidelines. Mice were genotyped by PCR amplification as previously described (Copley et al., 2013; Ravni et al., 2009).

Immunofluorescence

Inner ears were fixed for 2 hours in a solution of 4% paraformaldehyde prepared in 67mM Sorenson's phosphate buffer (pH 7.4). For immunofluorescent labeling, inner ear sensory organs were micro-dissected to expose the sensory epithelia and permeabilized and blocked using blocking solution (5% donkey serum, 1% BSA, and PBS) supplemented with Triton X-100 to 0.5%. Primary antibodies and phalloidin Alexa Fluor 488 (Invitrogen A12379) were diluted in blocking solution supplemented with Tween-20 to 0.1% and incubated with the tissue overnight at 4°C. Tissue was washed thoroughly with PBS-T (PBS and 0.05% Tween-20), followed by incubation with species-specific, Alexa Fluor-conjugated (Invitrogen) or DyLight-conjugated (Jackson ImmunoResearch) secondary antibodies. Tissue was subsequently washed with PBS-T, mounted using Prolong Gold (Molecular Probes, P36930), and imaged via structured illumination microscopy using a Zeiss Axio Imager M.2 with ApoTome.2 attachment. Images were collected with Zeiss Zen software, and figures were prepared with Adobe Illustrator. The following commercial antibodies were used in this study: β2-Spectrin (BD Biosciences 612562); Oncomodulin (Santa Cruz Sc7446). The Celsr1 antibody was provided by D. Devenport and has been previously described (Devenport and Fuchs, 2008).

Quantification of hair cell orientation

For measuring and quantifying the orientation of vestibular stereociliary bundles, utricular maculae and horizontal cristae were immunolabeled using antibodies against β2-Spectrin and imaged at 63x magnification as previously described. Stereociliary bundle orientation was determined based upon the polarized position of the fonticulus (see Figure 1), with orientation vectors extending from the center of the cuticular plate to the fonticulus, and a

user defined reference-line drawn along the lateral border of the sensory epithelia (see Figure 9&10). Measurements and graphing were conducted using customized software developed in Python which generated orientation vectors based upon manually annotated positions of the fonticulus and cuticular plate center. To measure bundle orientation the software generated a second line tangential to the user defined reference-line, and at a point aligned with the x-position of the cell center. Using this approach, bundle orientation is the measured angle between the orientation vector and the tangent of the reference-line. As a result, when graphed on a circular histogram 90° is a stereociliary bundle orientation that is perpendicular to the reference-line. For the semi-circular canal cristae, measurements were obtained from hair cells located within the center of the sensory epithelium. Measurements were pooled from a single crista from 3 *Celsr1* KOs and littermate controls for horizontal and anterior cristae, while the posterior measurements were gathered from 2 *Celsr1* KOs and 2 littermate controls. For the utricular maculae measurements were obtained from hair cells located in three distinct regions and separate circular histograms were created for each. Regions were identified based upon immunolabeling for the striola marker Oncomodulin, and measurements were pooled within each region for utricles from 4 *Celsr1* KOs or 2 littermate controls.

For measuring and quantifying the orientation of auditory hair cells within the organ of Corti, cochleas were labeled with phalloidin and an antibody against β2-Spectrin to determine the location of the fonticulus. Stereociliary bundle orientation was determined based upon the polarized position of the fonticulus relative to the neural:abneural axis, with 0° corresponding to a hair cell with the fonticulus on the abneural side and on this axis. Hair cells with a fonticulus deviating >30° from the neural:abneural axis were characterized as misoriented. Hair cells were manually scored for misorientation by comparison to a 30° template.

Supplementary Material

Refer to Web version on PubMed Central for supplementary material.

Acknowledgments

We would like to thank Orvelin Roman for his assistance with mouse colony maintenance. This work was supported by NIH/NIDCD grants R01 DC013066 (MRD) and F32 DC014390 (JSD).

References

Abraira VE, Del Rio T, Tucker AF, Slonimsky J, Keirnes HL, Goodrich LV. Cross-repressive interactions between Lrig3 and netrin 1 shape the architecture of the inner ear. Development. 2008; 135:4091–4099. [PubMed: 19004851]

Bastock R, Strutt H, Strutt D. Strabismus is asymmetrically localised and binds to Prickle and Dishevelled during Drosophila planar polarity patterning. Development. 2003; 130:3007–3014. [PubMed: 12756182]

Chae J, Kim MJ, Goo JH, Collier S, Gubb D, Charlton J, Adler PN, Park WJ. The Drosophila tissue polarity gene starry night encodes a member of the protocadherin family. Development. 1999; 126:5421–5429. [PubMed: 10556066]

Chen WS, Antic D, Matis M, Logan CY, Povelones M, Anderson GA, Nusse R, Axelrod JD. Asymmetric homotypic interactions of the atypical cadherin flamingo mediate intercellular polarity signaling. Cell. 2008; 133:1093–1105. [PubMed: 18555784]

Copley CO, Duncan JS, Liu C, Cheng H, Deans MR. Postnatal refinement of auditory hair cell planar polarity deficits occurs in the absence of Vangl2. The Journal of neuroscience: the official journal of the Society for Neuroscience. 2013; 33:14001–14016. [PubMed: 23986237]

Copp AJ, Greene ND, Murdoch JN. The genetic basis of mammalian neurulation. Nature reviews Genetics. 2003; 4:784–793.

Cryns K, van Alphen AM, van Spaendonck MP, van de Heyning PH, Timmermans JP, de Zeeuw CI, van Camp G. Circling behavior in the Ecl mouse is caused by lateral semicircular canal defects. J Comp Neurol. 2004; 468:587–595. [PubMed: 14689488]

Curtin JA, Quint E, Tsipouri V, Arkell RM, Cattanach B, Copp AJ, Henderson DJ, Spurr N, Stanier P, Fisher EM, Nolan PM, Steel KP, Brown SDM, Gray IC, Murdoch JN. Mutation of Celsr1 Disrupts Planar Polarity of Inner Ear Hair Cells and Causes Severe Neural Tube Defects in the Mouse. Current Biology. 2003; 13:1129–1133. [PubMed: 12842012]

Davies A, Formstone C, Mason I, Lewis J. Planar polarity of hair cells in the chick inner ear is correlated with polarized distribution of c-flamingo-1 protein. Dev Dyn. 2005; 233:998–1005. [PubMed: 15830377]

Deans MR. A balance of form and function: planar polarity and development of the vestibular maculae. Seminars in cell & developmental biology. 2013; 24:490–498. [PubMed: 23507521]

Deans MR, Antic D, Suyama K, Scott MP, Axelrod JD, Goodrich LV. Asymmetric distribution of prickle-like 2 reveals an early underlying polarization of vestibular sensory epithelia in the inner ear. J Neurosci. 2007; 27:3139–3147. [PubMed: 17376975]

Devenport D, Fuchs E. Planar polarization in embryonic epidermis orchestrates global asymmetric morphogenesis of hair follicles. Nature cell biology. 2008; 10:1257–1268. [PubMed: 18849982]

Dong S, Leung KK, Pelling AL, Lee PY, Tang AS, Heng HH, Tsui LC, Tease C, Fisher G, Steel KP, Cheah KS. Circling, deafness, and yellow coat displayed by yellow submarine (ysb) and light coat and circling (lcc) mice with mutations on chromosome 3. Genomics. 2002; 79:777–784. [PubMed: 12036291]

Ezan J, Lasvaux L, Gezer A, Novakovic A, May-Simera H, Belotti E, Lhoumeau AC, Birnbaumer L, Beer-Hammer S, Borg JP, Le Bivic A, Nurnberg B, Sans N, Montcouquiol M. Primary cilium migration depends on G-protein signalling control of subapical cytoskeleton. Nature cell biology. 2013; 15:1107–1115. [PubMed: 23934215]

Gibson F, Walsh J, Mburu P, Varela A, Brown KA, Antonio M, Beisel KW, Steel KP, Brown SD. A type VII myosin encoded by the mouse deafness gene shaker-1. Nature. 1995; 374:62–64. [PubMed: 7870172]

Giese AP, Ezan J, Wang L, Lasvaux L, Lembo F, Mazzocco C, Richard E, Reboul J, Borg JP, Kelley MW, Sans N, Brigande J, Montcouquiol M. Gipc1 has a dual role in Vangl2 trafficking and hair bundle integrity in the inner ear. Development. 2012; 139:3775–3785. [PubMed: 22991442]

Goodrich LV, Strutt D. Principles of planar polarity in animal development. Development. 2011; 138:1877–1892. [PubMed: 21521735]

Greene ND, Stanier P, Copp AJ. Genetics of human neural tube defects. Hum Mol Genet. 2009; 18:R113–129. [PubMed: 19808787]

Lu B, Usui T, Uemura T, Jan L, Jan YN. Flamingo controls the planar polarity of sensory bristles and asymmetric division of sensory organ precursors in Drosophila. Current biology: CB. 1999; 9:1247–1250. [PubMed: 10556092]

Lu X, Borchers AG, Jolicoeur C, Rayburn H, Baker JC, Tessier-Lavigne M. PTK7/CCK-4 is a novel regulator of planar cell polarity in vertebrates. Nature. 2004; 430:93–98. [PubMed: 15229603]

Montcouquiol M, Rachel RA, Lanford PJ, Copeland NG, Jenkins NA, Kelley MW. Identification of Vangl2 and Scrb1 as planar polarity genes in mammals. Nature. 2003; 423:173–177. [PubMed: 12724779]

Montcouquiol M, Sans N, Huss D, Kach J, Dickman JD, Forge A, Rachel RA, Copeland NG, Jenkins NA, Bogani D, Murdoch J, Warchol ME, Wenthold RJ, Kelley MW. Asymmetric localization of

Vangl2 and Fz3 indicate novel mechanisms for planar cell polarity in mammals. J Neurosci. 2006; 26:5265–5275. [PubMed: 16687519]

Ohyama T, Groves AK. Generation of Pax2-Cre mice by modification of a Pax2 bacterial artificial chromosome. Genesis. 2004; 38:195–199. [PubMed: 15083520]

Ravni A, Qu Y, Goffinet AM, Tissir F. Planar cell polarity cadherin Celsr1 regulates skin hair patterning in the mouse. J Invest Dermatol. 2009; 129:2507–2509. [PubMed: 19357712]

Schwander M, Kachar B, Muller U. Review series: The cell biology of hearing. The Journal of cell biology. 2010; 190:9–20. [PubMed: 20624897]

Shotwell SL, Jacobs R, Hudspeth AJ. Directional sensitivity of individual vertebrate hair cells to controlled deflection of their hair bundles. Ann N Y Acad Sci. 1981; 374:1–10.

Simons M, Mlodzik M. Planar cell polarity signaling: from fly development to human disease. Annu Rev Genet. 2008; 42:517–540. [PubMed: 18710302]

Song H, Hu J, Chen W, Elliott G, Andre P, Gao B, Yang Y. Planar cell polarity breaks bilateral symmetry by controlling ciliary positioning. Nature. 2010; 466:378–382. [PubMed: 20562861]

Struhl G, Casal J, Lawrence PA. Dissecting the molecular bridges that mediate the function of Frizzled in planar cell polarity. Development. 2012; 139:3665–3674. [PubMed: 22949620]

Strutt H, Strutt D. Differential stability of flamingo protein complexes underlies the establishment of planar polarity. Current biology: CB. 2008; 18:1555–1564. [PubMed: 18804371]

Tarchini B, Jolicoeur C, Cayouette M. A molecular blueprint at the apical surface establishes planar asymmetry in cochlear hair cells. Developmental cell. 2013; 27:88–102. [PubMed: 24135232]

Tissir F, Goffinet AM. Expression of planar cell polarity genes during development of the mouse CNS. The European journal of neuroscience. 2006; 23:597–607. [PubMed: 16487141]

Tissir F, Goffinet AM. Atypical cadherins Celsr1-3 and planar cell polarity in vertebrates. Prog Mol Biol Transl Sci. 2013; 116:193–214. [PubMed: 23481196]

Torban E, Patenaude AM, Leclerc S, Rakowiecki S, Gauthier S, Andelfinger G, Epstein DJ, Gros P. Genetic interaction between members of the Vangl family causes neural tube defects in mice. Proceedings of the National Academy of Sciences of the United States of America. 2008; 105:3449–3454. [PubMed: 18296642]

Uchino Y, Kushiro K. Differences between otolith- and semicircular canal-activated neural circuitry in the vestibular system. Neurosci Res. 2011; 71:315–327. [PubMed: 21968226]

Usui T, Shima Y, Shimada Y, Hirano S, Burgess RW, Schwarz TL, Takeichi M, Uemura T. Flamingo, a seven-pass transmembrane cadherin, regulates planar cell polarity under the control of Frizzled. Cell. 1999; 98:585–595. [PubMed: 10490098]

Vladar EK, Antic D, Axelrod JD. Planar cell polarity signaling: the developing cell's compass. Cold Spring Harbor perspectives in biology. 2009; 1:a002964. [PubMed: 20066108]

Wang J, Hamblet NS, Mark S, Dickinson ME, Brinkman BC, Segil N, Fraser SE, Chen P, Wallingford JB, Wynshaw-Boris A. Dishevelled genes mediate a conserved mammalian PCP pathway to regulate convergent extension during neurulation. Development. 2006a; 133:1767–1778. [PubMed: 16571627]

Wang Y, Guo N, Nathans J. The role of Frizzled3 and Frizzled6 in neural tube closure and in the planar polarity of inner-ear sensory hair cells. J Neurosci. 2006b; 26:2147–2156. [PubMed: 16495441]

Wang Y, Nathans J. Tissue/planar cell polarity in vertebrates: new insights and new questions. Development. 2007; 134:647–658. [PubMed: 17259302]

Wang Y, Williams J, Rattner A, Wu S, Bassuk AG, Goffinet AM, Nathans J. Patterning of papillae on the mouse tongue: A system for the quantitative assessment of planar cell polarity signaling. Developmental biology. 2016; 419:298–310. [PubMed: 27612405]

Yates BJ, Bolton PS, Macefield VG. Vestibulo-sympathetic responses. Comprehensive Physiology. 2014; 4:851–887. [PubMed: 24715571]

Yin H, Copley CO, Goodrich LV, Deans MR. Comparison of phenotypes between different vangl2 mutants demonstrates dominant effects of the Looptail mutation during hair cell development. PLoS One. 2012; 7:e31988. [PubMed: 22363783]

Highlights

- *Celsr1* knockout mice have vestibular behavior phenotypes
- Celsr1 is asymmetrically distributed at cell boundaries between hair cells and supporting cells
- Celsr1 asymmetric distribution is correlated with stereociliary bundle orientation
- *Celsr1* knockout mice have misoriented vestibular stereociliary bundles

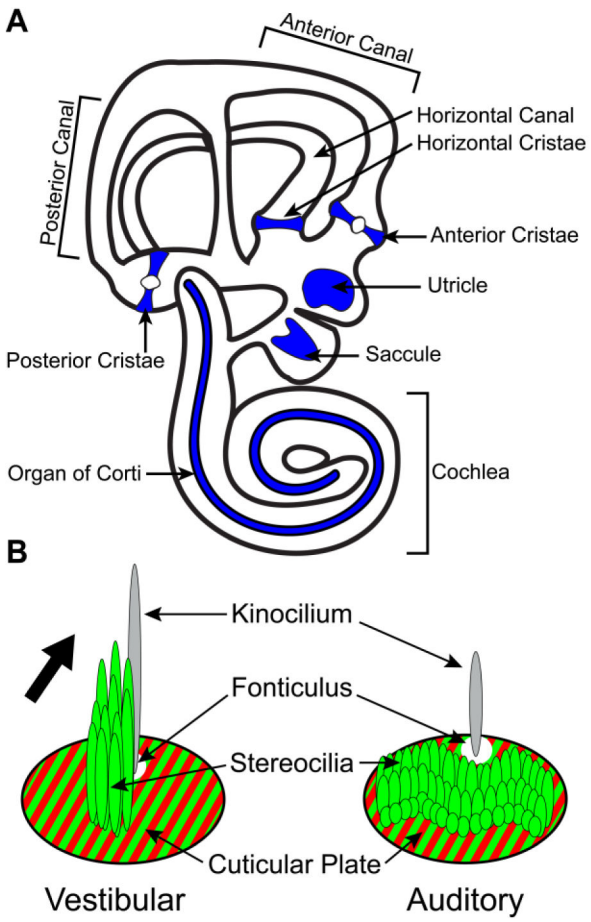

Figure 1. Anatomical organization of the mouse inner ear and hair cell stereociliary bundles

(A) Sensory receptor hair cells are distributed between six sensory organs demarcated by blue shading in this diagrammatic representation of the mouse inner ear. Three vestibular organs, the anterior cristae, posterior cristae and horizontal cristae are associated with the semi-circular canals and detect rotational movements. The anterior and posterior cristae can be distinguished in part by the presence of the eminentia cruciatum, a central region consisting of non-sensory epithelia that is devoid of hair cells, and is not found in the horizontal cristae. Two additional vestibular organs, the utricle and saccule, detect gravity and linear acceleration in the horizontal and vertical planes respectively. A single auditory organ called the organ of Corti detects sound and spirals along the length of the cochlea. **(B)** The stereociliary bundle of an individual hair cell consists of a staircase array of stereocilia arranged with the tallest adjacent to the kinocilium. The stereocilia are embedded within an actin meshwork called the cuticular plate which is located throughout the apical surface of the hair cell with the exception of a small region where the kinocilium is anchored to an underlying basal body. The cuticular plate can be labeled using antibodies against β2-Spectrin (red) and outlines the fonticulus; the anchorage site of the kinocilium which can be used to visualize stereociliary bundle orientation. Flourescently-tagged phalloidin (green) labels filamentous actin in the stereocilia and cuticular plate as well as intercellular junctions (not illustrated). Hair cells of the vestibular sensory epithelia and auditory hair cells of the

cochlea differ in the organization and length of stereocilia yet both have a distinct planar polarity that is evident in the morphology of the stereociliary bundle and the position of the fonticulus. The orientation of the vestibular stereociliary bundle is indicated by the large black arrow.

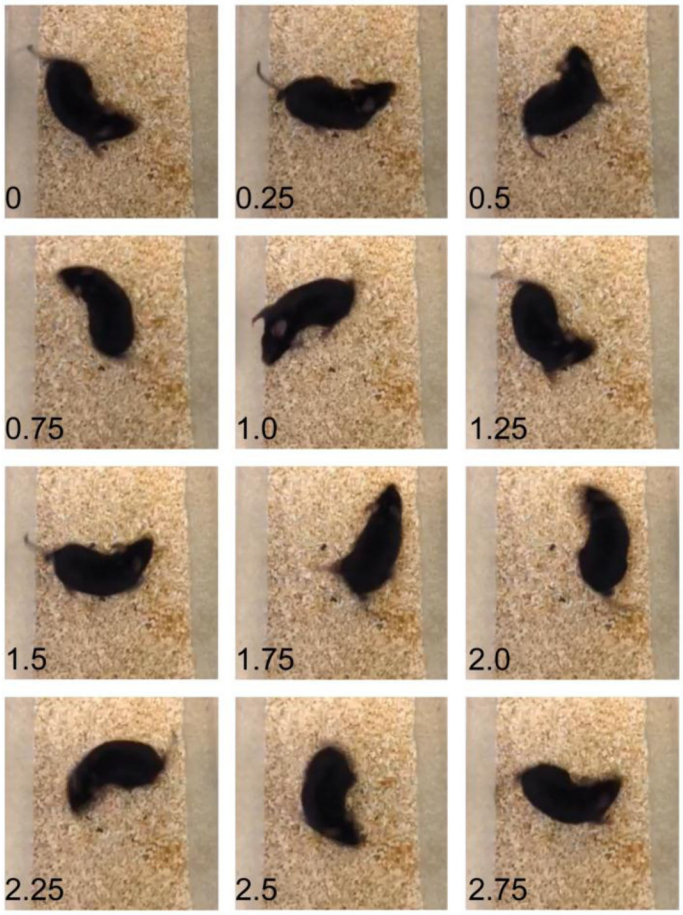

Figure 2. Targeted deletion of *Celsr1* results in circling behavior indicative of vestibular deficits

Still frame images isolated from a video of the spontaneous navigational behavior of a *Celsr1* knockout mouse. Individual still images from this video at 0.25 second intervals illustrates a circling bout lasting approximately 3 seconds. The full length video is available as a supplemental movie.

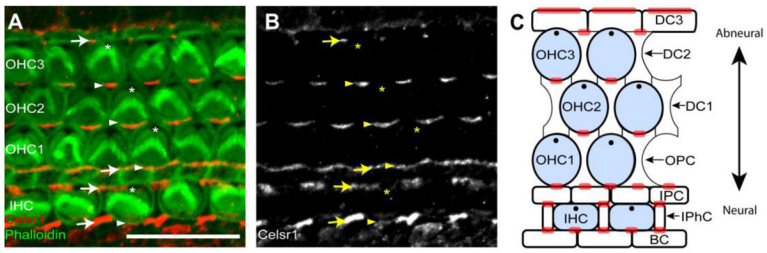

Figure 3. Celsr1 is asymmetrically distributed at cell boundaries in the developing Organ of Corti of the cochlea

(A) Celsr1 immunofluorescence (red) and phalloidin labeling (green) shows Celsr1 distribution in the organ of Corti of the mouse cochlea at P2. Celsr1 is enriched at the neural boundary of outer hair cells at the junction with the adjacent supporting cell. **(B)** Grayscale image of Celsr1 immunoflourescent labeling from 'A'. Arrowheads illustrate examples of Celsr1 at HC:SC boundaries, arrows illustrate examples of Celsr1 at SC:SC boundaries and asters mark the position of the fonticulus in a subset of hair cells. **(C)** Schematic diagram summarizing the distribution of Celsr1 relative to the different cell types of the organ of Corti. Hair cells are blue and red shading shows the relative distribution of Celsr1 at cell boundaries based upon the immunofluorescent labeling in 'A'. IHC (Inner Hair Cell), OHC (Outer Hair Cell), DC (Deiters' cell), IPC (Inner Pillar Cell), OPC (Outer Pillar Cell), IPhC (Inter Phalangeal Cell), BC (Border Cell). Anatomical reference arrow points along the neural to abneural axis of the inner ear. Scale bar, 10μm.

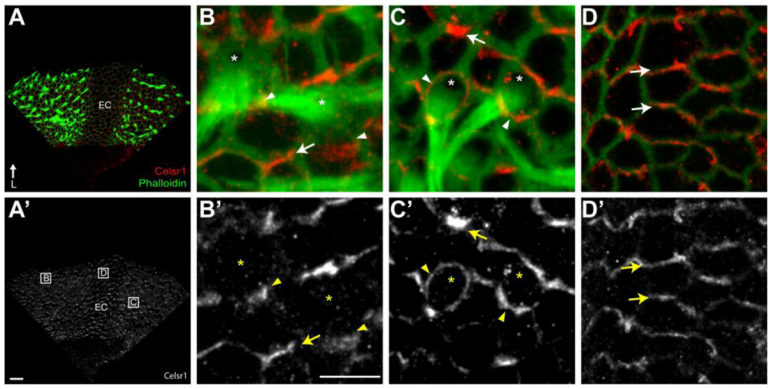

Figure 4. Celsr1 is Asymmetrically Localized in the Developing Cristae

(A) The anterior cristae at P2 contains two fields of hair cells that can be visualized using phalloidin (green), flank the eminentia cruciatum (EC), and contains Celsr1 (red) at cell boundaries throughout. **(A′)** Grayscale image of Celsr1 immunofluorescent labeling from 'A'. Boxed fields correspond to approximate locations of higher magnification images in panels 'B–D'. **(B,B′)** Celsr1 is localized to HC:SC boundaries and SC:SC boundaries in the sensory epithelia of the cristae. **(C,C′)** A subset of hair cells are surrounded by Celsr1 which is present at the boundaries with all adjacent supporting cells. **(D,D′)** Celsr1 distribution in non-sensory cells of the EC is also asymmetric and resembles the distribution at SC:SC boundaries. **(B–D)** Arrowheads illustrate examples of Celsr1 at HC:SC boundaries, arrows illustrate examples of Celsr1 at SC:SC boundaries and asters mark the position of the fonticulus in a subset of hair cells. Anatomical reference arrow points along the Lateral (L) axis of the inner ear. Scale bars are 20 μm in 'A', 10μm in 'B'.

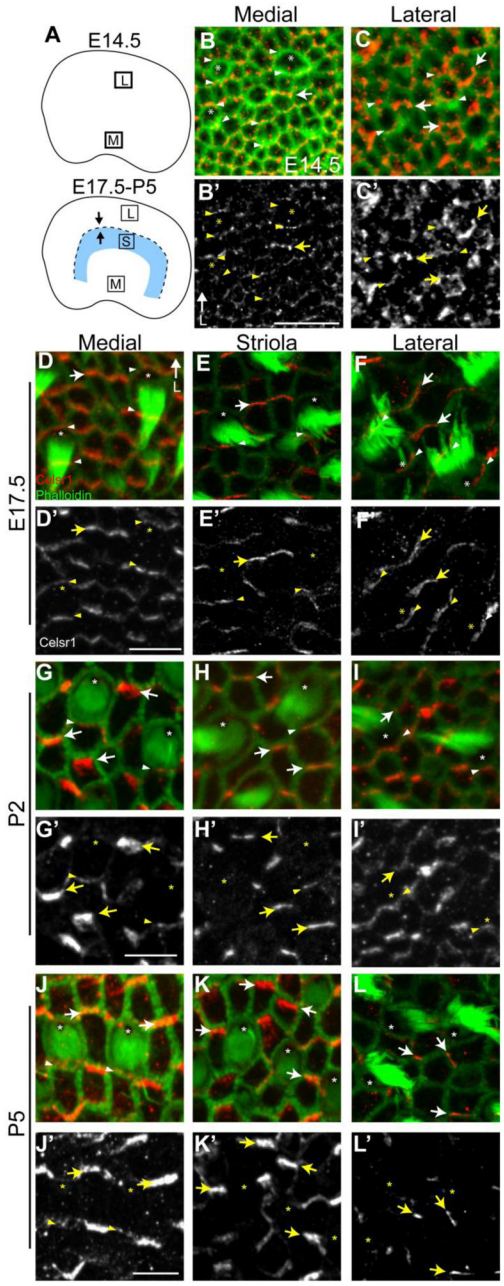

Figure 5. Celsr1 is asymmetrically localized and dynamically regulated in the developing vestibular sensory epithelia

(A) Schematic diagrams of the utricular maculae at early (E14.5) and later (E17.5 – P5) stages of development showing the approximate locations of medial (M), lateral (L) and striolar (S) imaging fields used throughout the figure. The LPR appears at later stages and is represented by a dashed line while arrows show relative stereociliary bundle orientation. **(B,C)** Celsr1 (red) and phalloidin (green) labeling of the E14.5 utricle demonstrates the asymmetric distribution of Celsr1 in medial imaging fields (B) where hair cells are beginning to differentiate and the lateral imaging field (C) which lack polarized stereociliary bundles at this stage. **(D–F)** At E17.5 Celsr1 is enriched at HC:SC and SC:SC boundaries

throughout the utricular maculae. In the medial imaging field Celsr1 is present at the cell boundaries along two sides of the hair cell. In contrast, in the striola and lateral imaging fields Celsr1 is restricted to the HC:SC boundary at the medial side of the hair cell. This medial distribution does not change between the striola and lateral regions despite the difference in stereociliary bundle orientation for hair cells on opposite sides of the LPR. **(G–I)** At P2 Celsr1 levels are decreasing at HC:SC boundaries throughout the utricular maculae and is only detected at boundaries on the medial side of hair cells. **(J–L)** By P5, Celsr1 is largely restricted to SC:SC boundaries and can only be found occasionally at HC:SC boundaries that are restricted to the medial imaging field (J) where levels are also significantly reduced compared to adjacent SC:SC boundaries. Arrowheads illustrate examples of Celsr1 at HC:SC boundaries, arrows illustrate examples of Celsr1 at SC:SC boundaries and asters mark the position of the fonticulus in a subset of hair cells. Anatomical reference arrow points along the Lateral (L) axis of the inner ear. Scale bars are 20μm.

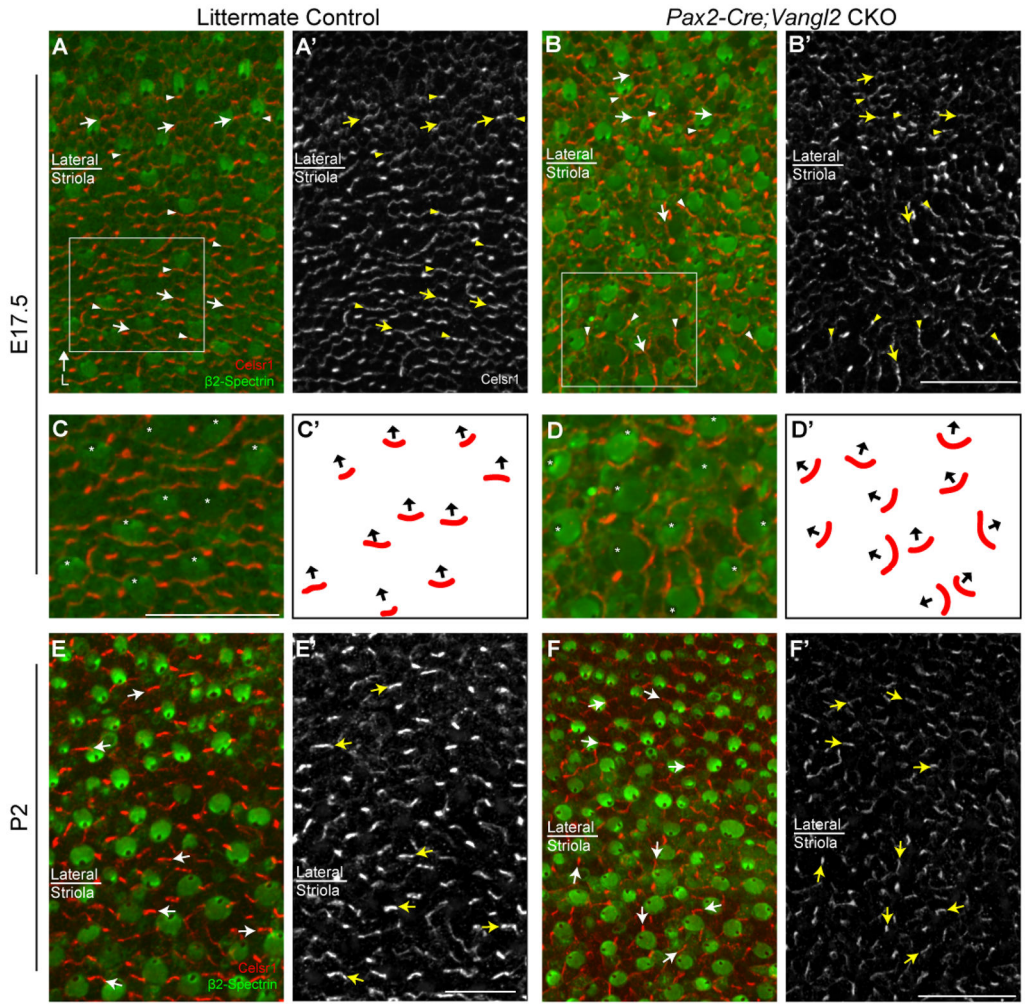

Figure 6. The polarized distribution of Celsr1 correlates with the axis of stereociliary bundle orientation in Vangl2 CKOs

(A) Celsr1 (red) and β2-Spectrin (green) immunofluorescent labeling of the utricle from an E17.5 littermate control mouse in a region spanning the boundary between the striola and lateral region. Celsr1 is localized to HC:SC boundaries at the medial side of hair cells irrespective of their position relative to the LPR. **(A′)** Grayscale image of Celsr1 immunoflourescent labeling from 'A'. **(B)** Celsr1 and β2-Spectrin labeling of the utricle from an E17.5 *Pax2*-Cre; *Vangl2* CKO mouse. Stereociliary bundles in the striolar region are misoriented relative to each other which is characteristic of the *Vangl2* KO phenotype. Bundle orientation can be inferred from the position of the fonticulus in the β2-Spectrin labeled hair cell apical surface. **(B′)** Grayscale image of Celsr1 immunofluorescent labeling from 'B'. Celsr1 remains asymmetric in the absence of Vangl2, however the polarized distribution is no longer coordinated between different cells in the striola while remaining organized in the lateral region. Boxed fields in 'A&B' correspond to approximate locations of higher magnification images in panels 'C&D' respectively. **(C)** Higher magnification images of E17.5 hair cells from 'A' in which the fonticulus is marked with an aster to illustrate stereociliary bundle orientation. In each of these hair cells Celsr1 is localized to the

HC:SC boundary opposite of the fonticulus. **(D)** Higher magnification images of *Pax2*-Cre; *Vangl2* CKO hair cells from 'B' showing the distribution of Celsr1 relative to misoriented stereociliary bundles. Celsr1 is maintained at the cell boundary opposite of the fonticulus. **(C′,D′)** Schematic representation of stereociliary bundle orientations and the relative position of Celsr1 for the hair cells imaged in 'E&F'. In these schematics, black arrows originate from the center of the apical cell surface and terminate at the fonticulus. **(E–F)** Salient features of the Celsr1 distribution pattern are maintained in the *Pax2*-Cre; *Vangl2* CKO at postnatal (P2) stages. While Celsr1 is downregulated at HC:SC junctions it remains prominent at SC:SC junctions, and the polarized distribution of Celsr1 at these junctions remains correlated with the orientation of stereociliary bundles on the adjacent hair cells. In all image panels except C′-D′, arrowheads illustrate examples of Celsr1 at HC:SC boundaries, arrows illustrate examples of Celsr1 at SC:SC boundaries and asters mark the position of the fonticulus in a subset of hair cells. Anatomical reference arrow points along the Lateral (L) axis of the inner ear, and is consistent for all images. Scale bars are 20 μm.

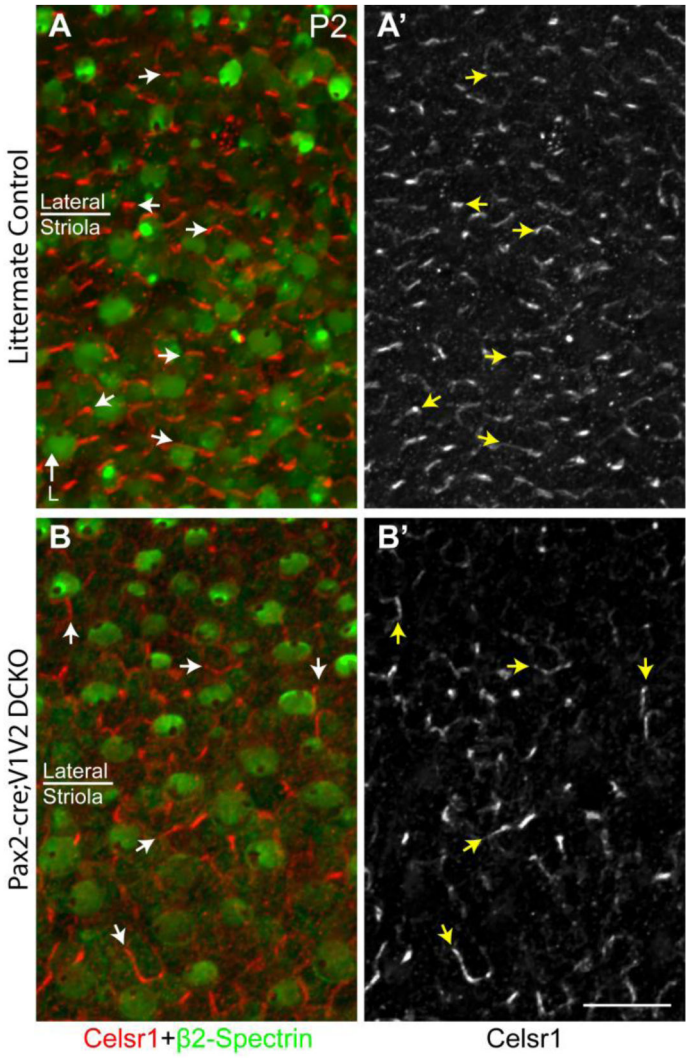

Figure 7. The polarized distribution of Celsr1 persists in the absence of Vangl1 and Vangl2

(A) Celsr1 (red) and β2-Spectrin (green) labeling of the utricle from P2 littermate control mouse in a region spanning the boundary between the striolar and lateral region. Celsr1 is localized to SC:SC boundaries and organized along an axis parallel to stereociliary bundle orientation. **(A′)** Grayscale image of Celsr1 immunoflourescent labeling from 'A'. **(B)** Celsr1 and β2-Spectrin labeling of the utricle from P2 *Pax2*-Cre; *Vangl1; Vangl2* CKO mouse. Stereociliary bundles are misoriented relative to each other in all regions consistent with the loss of PCP signaling throughout the maculae. Bundle orientation can be inferred from the position of the fonticulus in the β2-Spectrin labeled hair cell apical surface. **(B′)** Grayscale image of Celsr1 immunoflourescent labeling from 'A'. Despite the loss of Vangl1 and Vangl2, Celsr1 is still found to be asymmetrically localized at SC:SC junctions but no longer appears coordinated with stereociliary bundle polarity. Arrowheads illustrate examples of Celsr1 at HC:SC boundaries, arrows illustrate examples of Celsr1 at SC:SC boundaries. Anatomical reference arrow points along the Lateral (L) axis of the inner ear. Scale bar is 20μm.

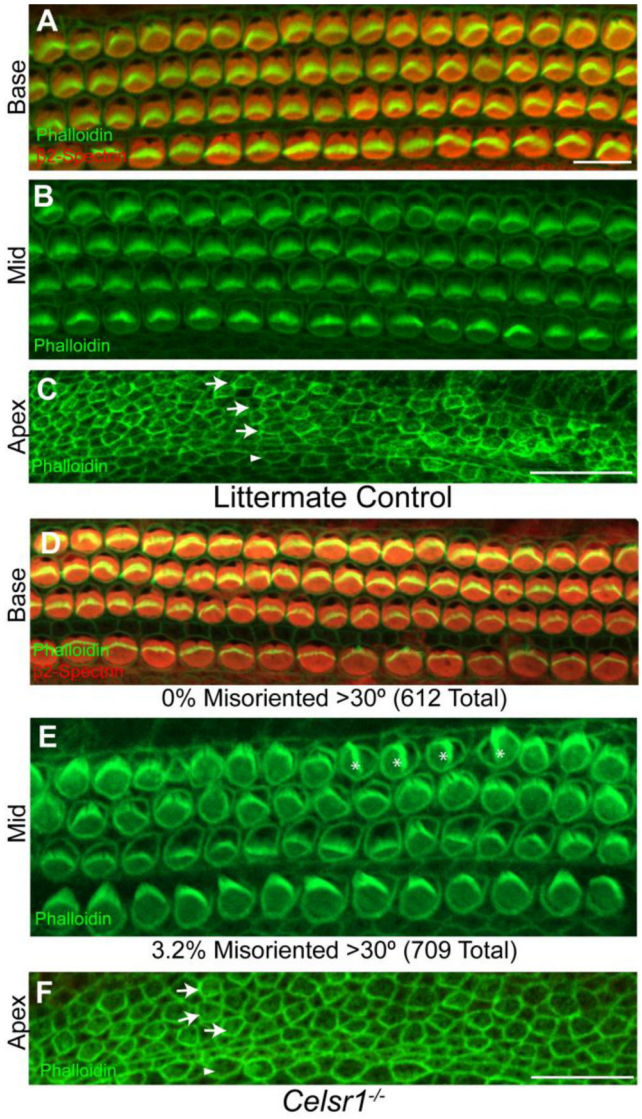

Figure 8. Celsr1 gene deletion has only mild effects on organ of Corti development

(A–C) β2-Spectrin (red) and phalloidin (green) labeling of auditory hair cells in the basal turn (A) or phalloidin labeling of hair cells in the middle turn (B) or apex (C) of the organ of Corti from littermate control cochleas at P0. All hair cells are oriented with the fonticulus towards the abneural edge of the organ of Corti, and in all regions a single row of IHCs and three rows of OHCs can be distinguished from the surrounding supporting cells. In the extreme apex (C) hair cells are less differentiated and have poorly formed stereocilia, but are still morphologically distinct from the surrounding supporting cells. **(D–F)** In the *Celsr1* KO cochlea, the orientation and patterning of auditory hair cells is similar to littermate controls in all regions. Only a small percentage (3.2%) of third row OHCs are misoriented >30°, and these are more prevalent in the middle but not the basal turn of the cochlea. *Celsr1* KO hair cells with misoriented stereociliary bundles are marked with asters (E). Arrows specify the position of the three rows of OHCs in the apex of littermate control (C) and *Celsr1* KO (F) cochlea. Arrowheads specify the position of the single row of IHCs. Scale bars are 20 μm.

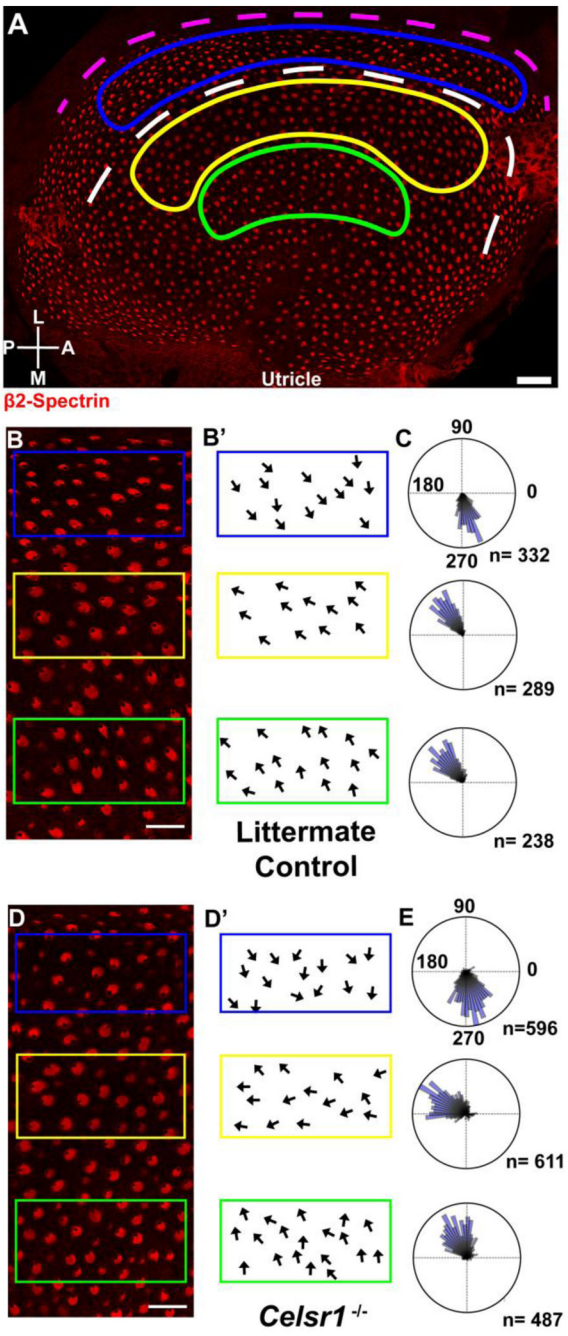

Figure 9. *Celsr1* gene deletion results in misoriented stereociliary bundles in the utricular maculae

(A) P0 littermate control utricle with hair cells labeled for β2-Spectrin (red) that has been annotated to illustrate the approximate position of the LPR (white dashed line), and the striolar (yellow), lateral extrastriolar (blue), and medial extrastriolar regions (green) used for quantification of stereociliary bundle orientation. Immunolabeling using antibodies against Oncomodulin was used to determine the position of the striola (data not shown). The dashed magenta line follows the lateral edge of the utricle and is used as a reference for polarity measurements as described in greater detail in the methods. **(B)** Higher magnification

images of utricular hair cells from littermate control mice labeled with β2-spectrin for quantification analysis. **(B′)** Schematic illustration of stereociliary bundle orientation from each of the three analysis fields outlined in 'B'. Arrows originate from the center of the apical cell surface and terminate at the fonticulus. **(C)** Circular histograms demonstrating cumulative stereociliary bundle orientations for hair cells from 2 littermate control utricles. The number of hair cells (n) contributing to each histogram are indicated. Measurements of 90° or 270° are perpendicular to the magenta reference line drawn in 'A'. **(D)** Higher magnification images of utricular hair cells from P0 *Celsr1* KO mice labeled with β2-spectrin for quantification analysis. **(D′)** Schematic illustration of stereociliary bundle orientation from each of the three analysis fields outlined in 'D'. **(E)** Circular histograms demonstrating cumulative stereociliary bundle orientations for hair cells from 4 *Celsr1* KO utricles. The number of hair cells (n) contributing to each histogram are indicated. Scale bars are 40μm in 'A', and 20μm in 'B' and 'D'.

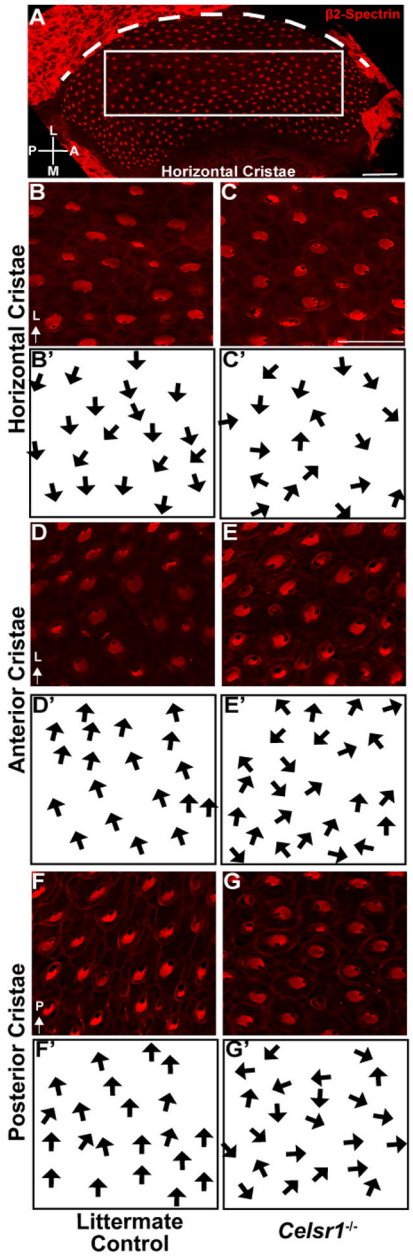

Figure 10. ***Celsr1*** **gene deletion results in misoriented stereociliary bundles in semi-circular canal cristae**

(A) P0 littermate control horizontal canal cristae with hair cells labeled for β2-Spectrin (red) that has been annotated to illustrate the location of a field of cells used for quantification of stereociliary bundle orientation. The dashed magenta line follows the lateral edge of the cristae and is used as a reference for polarity measurements. **(B)** Higher magnification image of horizontal canal cristae hair cells from within the analysis field of littermate control mice labeled with β2-Spectrin. **(B′)** Schematic illustration of stereociliary bundle orientation from hair cells in 'B'. In the horizontal canal cristae stereociliary bundles are oriented medially and towards the adjacent utricle. **(C)** Higher magnification image of cristae hair cells from

P0 *Celsr1* KO mouse labeled with β2-Spectrin for quantification analysis. **(C′)** Schematic illustration of stereociliary bundle orientation from hair cells in 'C'. **(D)** Higher magnification image of anterior canal cristae hair cells from littermate control mice labeled with β2-Spectrin. **(D′)** Schematic illustration of stereociliary bundle orientation from hair cells in 'D'. In the anterior canal cristae stereociliary bundles are oriented laterally and away from the adjacent utricle. **(E,E′)** Higher magnification image and schematic of anterior cristae hair cells from P0 *Celsr1* KO mouse. **(F,F′)** Higher magnification image and schematic of posterior cristae hair cells from at littermate control mouse. In the posterior canal cristae stereociliary bundles are oriented laterally and thus point away fromthe adjacent utricle. **(G,G′)** Higher magnification image and schematic of posterior cristae hair cells from P0 *Celsr1* KO mouse. In all schematic illustrations arrows originate from the center of the apical cell surface and terminate at the kinocilium. Anatomical reference arrows point along the Lateral (L) or Posterior (P) axes of the inner ear. Scale bars are 50μm in 'A' and 25μm in 'C'.

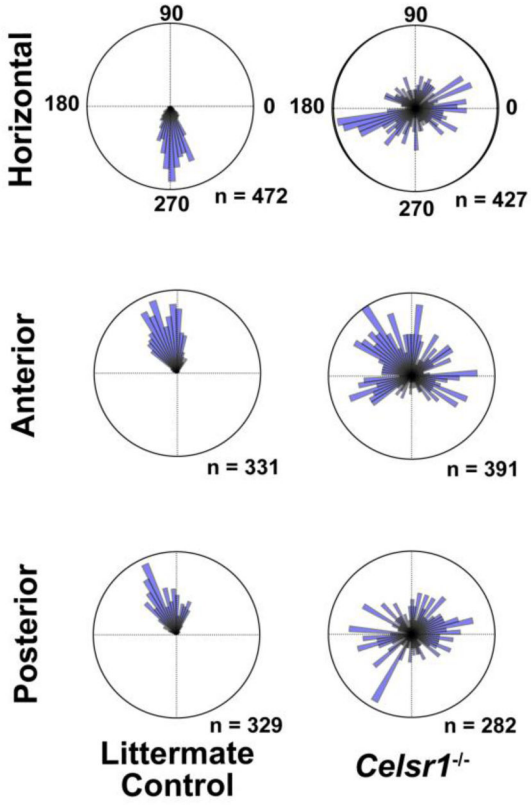

Figure 11. Quantification of stereociliary bundle orientation in control and *Celsr1* KO cristae

Circular histograms demonstrating cumulative stereociliary bundle orientations for hair cells from each of the semi-circular canal cristae. Graphs of the horizontal and anterior canal cristae are from 3 littermate control and 3 *Celsr1* KOs. Graphs of the posterior canal cristae are from 2 littermate controls and 2 *Celsr1* KOs. The number of hair cells (n) contributing to each histogram are indicated. Measurements of 90° or 270° are perpendicular to a reference line drawn along the border of the sensory epithelia as illustrated for the horizontal cristae in Figure 10A.